Active sites for ice nucleation differ depending on nucleation mode

Mark A. Holden[a,b,1,2], James M. Campbell[a,1,2], Fiona C. Meldrum[c], Benjamin J. Murray[d], and Hugo K. Christenson[a]

[a]School of Physics and Astronomy, University of Leeds, Leeds, LS2 9JT, United Kingdom; [b]School of Physical Sciences and Computing, University of Central Lancashire, Preston, PR1 2HE, United Kingdom; [c]School of Chemistry, University of Leeds, Leeds, LS2 9JT, United Kingdom; and [d]School of Earth and Environment, University of Leeds, Leeds, LS2 9JT, United Kingdom

Edited by Daan Frenkel, University of Cambridge, Cambridge, United Kingdom, and approved March 12, 2021 (received for review November 4, 2020)

The nucleation of ice crystals in clouds is poorly understood, despite being of critical importance for our planet's climate. Nucleation occurs largely at rare "active sites" present on airborne particles such as mineral dust, but the nucleation pathway is distinct under different meteorological conditions. These give rise to two key nucleation pathways where a particle is either immersed in a supercooled liquid water droplet (immersion freezing mode) or suspended in a supersaturated vapor (deposition mode). However, it is unclear if the same active sites are responsible for nucleation in these two modes. Here, we directly compare the sites that are active in these two modes by performing immersion freezing and deposition experiments on the same thin sections of two atmospherically important minerals (feldspar and quartz). For both substrates, we confirm that nucleation is dominated by a limited number of sites and show that there is little correlation between the two sets of sites operating in each experimental method: across both materials, only six out of 73 sites active for immersion freezing nucleation were also active for deposition nucleation. Clearly, different properties determine the activity of nucleation sites for each mode, and we use the pore condensation and freezing concept to argue that effective deposition sites have size and/or geometry requirements not of relevance to effective immersion freezing sites. Hence, the ability to nucleate is pathway dependent, and the mode of nucleation has to be explicitly considered when applying experimental data in cloud models.

nucleation | crystallization | ice | pores | active sites

Ice-containing clouds have a profound impact on climate (1–3). Our imperfect knowledge of their response to changing environmental conditions is a major source of uncertainty in models of our present and future climate, and a large part of this is due to limited understanding of fundamental ice nucleation processes (1, 2, 4, 5). We know that nucleation of ice in the atmosphere is dependent upon the presence of aerosol particles to provide suitable nucleation sites. However, our understanding of which aerosol particles in the atmosphere trigger ice formation, under what conditions, and how they do so remains poor.

One complicating factor is that the outcome of nucleation (the number, position, and orientation of crystals) cannot be assumed to depend simply upon the nucleation sites present and upon the conditions (the temperature and relative humidity). The pathway by which those conditions were achieved must also be considered, and there are at least two very distinct modes of nucleation which operate in the atmosphere. In higher temperature conditions, such as those typical in low-altitude mixed-phase clouds, the dominant pathway is freezing nucleation within a droplet of supercooled water that has condensed on or around a particle, termed immersion freezing (6, 7). However, at higher altitudes and lower temperatures, such as within a cirrus cloud, another process becomes important: so-called deposition nucleation. In this process, an ice crystal nucleates at a particle's surface without any prior condensation of bulk water (4, 7). These two pathways are illustrated in Fig. 1.

The mechanism by which deposition nucleation occurs has been much discussed (8–12). The traditional model is that ice crystals nucleate directly from the vapor (13), as suggested by the absence of a visible liquid phase when viewed under an optical microscope, and because deposition nucleation often occurs in conditions below water saturation in which bulk water could not condense. Alternatively, it has been suggested that nanoscale pores on the surface fill with supercooled water through capillary condensation and subsequently freeze (8), a model known as pore condensation and freezing. Evidence for such two-step nucleation via capillary condensation has been demonstrated by Christenson (11). A review of experimental data by Marcolli (9), coupled with experiments by Campbell et al. (12, 14) and David et al. (10), provide strong evidence that deposition nucleation of ice occurs through pore condensation and freezing. Throughout, we shall use the phrase "deposition nucleation" to indicate any ice nucleation from the vapor phase, whether true deposition or condensation and freezing of minute volumes of water.

Feldspar and quartz are two examples of minerals commonly found in the atmosphere which are known to be effective nucleants for both freezing and deposition nucleation of ice (15–17). Of the two, feldspars are typically able to nucleate ice at higher temperatures than quartz (18); feldspars rich in potassium (K-feldspars) are known to be particularly effective ice nucleants (15, 19–21). Studies of freezing nucleation of ice on feldspar and quartz have shown that nucleation is not uniform across the surface but is concentrated in a few rare "active sites" (22–24). This effect was also observed in deposition nucleation on feldspar, where nucleation favors certain topographic or crystallographic features

Significance

The appearance of ice crystals in the atmosphere is an important component of our planet's climate. Ice crystals usually form on solid particles suspended in the atmosphere, where a water droplet can either condense on the particle and then freeze, or ice can grow directly on the particle without water first condensing. However, understanding of why some types of particles are especially effective is poor. Here, we use microscopy to identify the sites where ice first forms on atmospherically important minerals and find a significant difference between the two modes of ice growth. These results provide insight into the factors that govern ice formation in the atmosphere and imply an important role of surface morphology in directing crystal formation.

Author contributions: M.A.H., F.C.M., B.J.M., and H.K.C. designed research; M.A.H. and J.M.C. performed research; M.A.H. and J.M.C. analyzed data; and M.A.H., J.M.C., F.C.M., B.J.M., and H.K.C. wrote the paper.

The authors declare no competing interest.

This article is a PNAS Direct Submission.

[1]M.A.H. and J.M.C. contributed equally to this work.

[2]To whom correspondence may be addressed. Email: mholden10@uclan.ac.uk or jamesmatthewcampbell@gmail.com.

This article contains supporting information online at https://www.pnas.org/lookup/suppl/doi:10.1073/pnas.2022859118/-/DCSupplemental.

Published April 26, 2021.

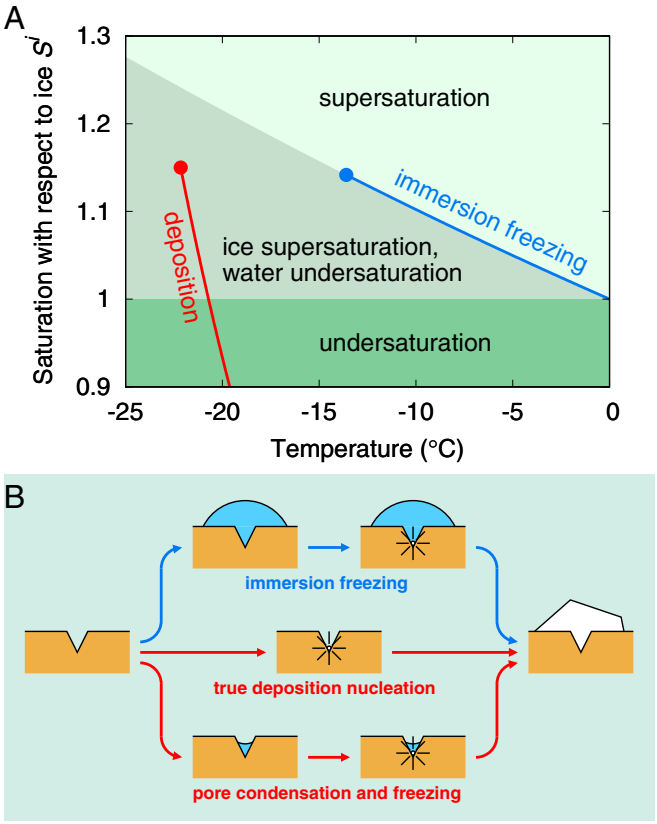

Fig. 1. Overview of the two modes of ice nucleation. (*A*) Representative pathways through temperature-saturation phase space. In immersion freezing, supercooled water follows the line of water saturation as temperature decreases, whereas in deposition experiments, the saturation of a body of gas increases rapidly with decreasing temperature once it is cooled below the frost point of the vapor (the temperature at intersection with the line $S^i = 1$). The circles represent the mean temperature and saturation at the moment when ice crystals were first observed in experiments on feldspar. (*B*) Schematic illustration of the two modes of growth. In immersion freezing, a bulk droplet of water condenses and is frozen following nucleation at an active site within the droplet. Two different models of deposition nucleation are illustrated. In true deposition nucleation, there is a direct vapor to solid nucleation event within an active site, leading to the growth of a bulk crystal. In pore condensation and freezing, a small volume of liquid condenses within a narrow geometry, which then freezes and grows into a bulk crystal.

(25, 26). Although such studies have done much to reveal the importance of active sites, almost all investigate either immersion freezing or deposition nucleation, not both. It has therefore not been possible to determine whether the activity of nucleation sites is mode specific or not or whether active sites for freezing nucleation are automatically active for deposition nucleation (or vice versa). This is a question which becomes more interesting if we assume a pore condensation and freezing explanation for deposition nucleation since it follows that nucleation involves a surface-induced freezing transition in both modes. It therefore seems plausible to expect a good degree of correlation between immersion freezing and deposition active sites.

In this paper, we investigate ice nucleation on thin sections of K-feldspar and quartz in order to determine whether the same active sites operate for both immersion freezing and deposition nucleation. Unlike the powdered mineral samples used in most studies, thin sections allow us to easily identify individual nucleation sites on the surface. It may not be immediately obvious why results obtained using millimeter-scaled thin sections are relevant for atmospheric aerosol particles. It is important to bear in mind that only a small fraction of dust particles in the atmosphere possess active sites at, say, −15 °C, but those few that do can dramatically alter cloud properties (5). The important quantity is the number of ice-active sites per unit surface area of dust, and in our experiments, we immerse an area of thin section of around 1 mm^2 in water and observe a single nucleation event. In the atmosphere, dust surface area varies massively, but in the dust-laden air off the coast of West Africa, there is on the order of 1 mm^2 of dust per liter of air (27), and hence, one active site would produce one ice crystal per liter of air—more than enough to influence cloud properties and initiate precipitation. In a previous study, we also showed that thin sections of feldspar have a similar density of active sites to powdered samples in immersion freezing experiments (22); hence, our results on thin sections are directly relevant for atmospheric mineral dust particles.

We used high-speed video microscopy to identify the dominant sites in a series of immersion freezing experiments, and deposition experiments were then carried out on the same areas to again identify the active sites. Our results demonstrate little correlation between the active sites for the two nucleation modes, which suggests different requirements for an effective nucleation site in each case.

Results

We performed immersion freezing and deposition nucleation experiments on 11 different regions across four feldspar thin sections polished along the (010) or (001) faces and on six different regions across three unpolished (100) facets of quartz. Deposition experiments were then carried out on the same regions of the same thin sections. The locations of nucleation events were recorded for each mode. Numerous repeat cycles of nucleation were performed on each region for each mode, allowing us to determine the most active sites for both freezing and deposition (we assume that two nucleation events on different cycles were the result of the same site if they were at the same position within experimental uncertainty). The two sets of identified active sites were then compared to determine any correlation. Here, we present results for each individual mode first before then presenting results of this comparison, in which we find a poor correlation, with only six out of 73 immersion freezing sites corresponding to one of the 337 deposition sites. *SI Appendix*, Table S1 also summarizes many of the results given below.

Immersion Freezing. Experiments were performed by pipetting a single droplet of water onto a quartz or feldspar surface (covering a surface area of 4 ± 1 mm^2) and then cooling until the droplet froze. High-speed microphotography was used to pinpoint the position of nucleation, and many repeat cycles of melting and refreezing the droplet were carried out to identify the distribution of nucleation sites across each surface.

Nucleation always occurred at one of a limited number of sites. For feldspar, a total of 222 freezing nucleation event locations were identified across 11 different droplets. These occurred at only 44 separate nucleation sites, and only two to seven sites were active within the area covered by each droplet. For quartz, 155 freezing events were pinpointed across six different droplets. These were associated with 34 unique nucleation sites, where between two and 11 sites operated in each droplet. Discounting the first cycle of each droplet, 84% of nucleation events on feldspar and 81% of nucleation events on quartz occurred at an already-identified nucleation site rather than a new site. These percentages would have been even higher had not the droplets been receding due to evaporation over the course of the experiment, which sometimes caused a dominant nucleation site to find itself outside the wetted area partway through an experiment. Nucleation is then forced to occur at other sites. In some drops, a single, highly active site triggers nucleation on every cycle (or until the edge of the droplet recedes past it), while in other areas, there are multiple sites of comparable activity with nucleation events stochastically distributed among them. The density of identified nucleation sites was

0.89 per mm^2 averaged across all droplets on feldspar and 1.4 per mm^2 on quartz.

Ice crystals on the (010) face of feldspar typically had a common epitaxial orientation of roughly rectangular appearance (Fig. 2*D*). This is consistent with previous results (22). This observation of epitaxy is important as it is definite evidence that nucleation occurred on surface features of the crystalline substrate rather than on contaminants on the surface or within the liquid. On the (001) face of feldspar, dendrites grew along curved trajectories, and the crystal orientations could not be inferred. On quartz, there was no consistent orientation, with hexagonal, rectangular, and spherical growth patterns all observed (Fig. 2 *A*–*C*). This inconsistent orientation suggests that epitaxy does not play an important role in determining the effectiveness of active sites on this substrate.

Freezing temperatures on feldspar were in the range −9.8 to −16.8 °C with a mean of −13.6 °C. Freezing temperatures on quartz were lower, being between −12.7 and −24.5 °C with a mean of −20.3 °C. To better compare the ice-nucleating activity of our thin sections to the powdered samples typically studied in the literature, a supporting set of experiments was performed by cooling an array of 1 µl water droplets on the substrates and observing the distribution of nucleation temperatures (*SI Appendix*, Fig. S1). Our four feldspar substrates all had similar efficacy, with median freezing temperatures between −10 and −12 °C, which is typical of this mineral once the nucleant surface area is normalized (19). For quartz, the medium nucleation temperature of −22 °C is lower than that typical for freshly ground quartz powders (18). This is attributed to a weathering effect, where it has previously been shown that the ice-nucleating ability of quartz decreases when in contact with water and air (18, 28). The surfaces used here were therefore more weathered than the freshly ground samples. Otherwise, the ability of these thin section samples to nucleate ice is consistent with powder suspensions.

Deposition. Deposition experiments were performed by maintaining an environment with fixed water vapor content while the temperature was decreased. Cooling below the temperature at which solid and vapor are in equilibrium (the frost point) results in supersaturated conditions under which ice nucleation can occur. In order to ensure nucleation of ice rather than droplets of supercooled water, it was found necessary to use frost points below typical nucleation temperatures in the immersion freezing experiments. The frost point was measured independently for every experiment and was −20.7 ± 0.5 °C (mean ± SD) for experiments with feldspar and −25.9 ± 0.4 °C for those with quartz. After nucleation was observed, the temperature was allowed to drop for a further 1.5 °C before being raised to above the melting point to remove the ice crystals. Six such cycles were performed on each area. The areas studied were the same as those examined in the immersion freezing experiments.

Nucleation on feldspar occurred in conditions below water saturation, while nucleation of quartz was seen in conditions very close to water saturation. Saturation with respect to ice (S^i) and water (S^w) at the first instance of nucleation on each cycle was $S^i = 1.15 \pm 0.07$ and $S^w = 0.93 \pm 0.05$ for feldspar (mean ± SD), and for quartz, $S^i = 1.30 \pm 0.03$ and $S^w = 0.98 \pm 0.02$.

In common with immersion freezing experiments, we again observed that a limited number of active sites dominated nucleation. Fig. 2 *E* and *F* shows an example of two cycles on the same feldspar substrate and reveals a good—although imperfect—degree of correlation between the two sets of nucleation sites. Altogether, 1,517 nucleation events were observed on feldspar at only 691 sites, and on quartz, 267 nucleation events were observed at 107 distinct sites. Discounting the first cycle for each region, 66% of nucleation events on feldspar and 74% of nucleation events on quartz occurred at an already-identified nucleation site rather than a new site. There was a lower density of nucleation on quartz than on feldspar, with an average of 1.6 crystals per mm^2 per cycle on quartz as compared to 5.8 crystals/mm^2 on feldspar, and across all cycles, an average density of identified nucleation sites of 15.7 per mm^2 on feldspar and 3.9 per mm^2 on quartz. These densities are much higher than in immersion freezing experiments due to the observation of multiple nucleation events per cycle rather than just one. The most active sites appeared to be the least common: typically, we observed a select few very active sites where nucleation occurred on every cycle at relatively low saturation and a much larger number of less active sites that produced crystals at relatively high saturation on one or two cycles only.

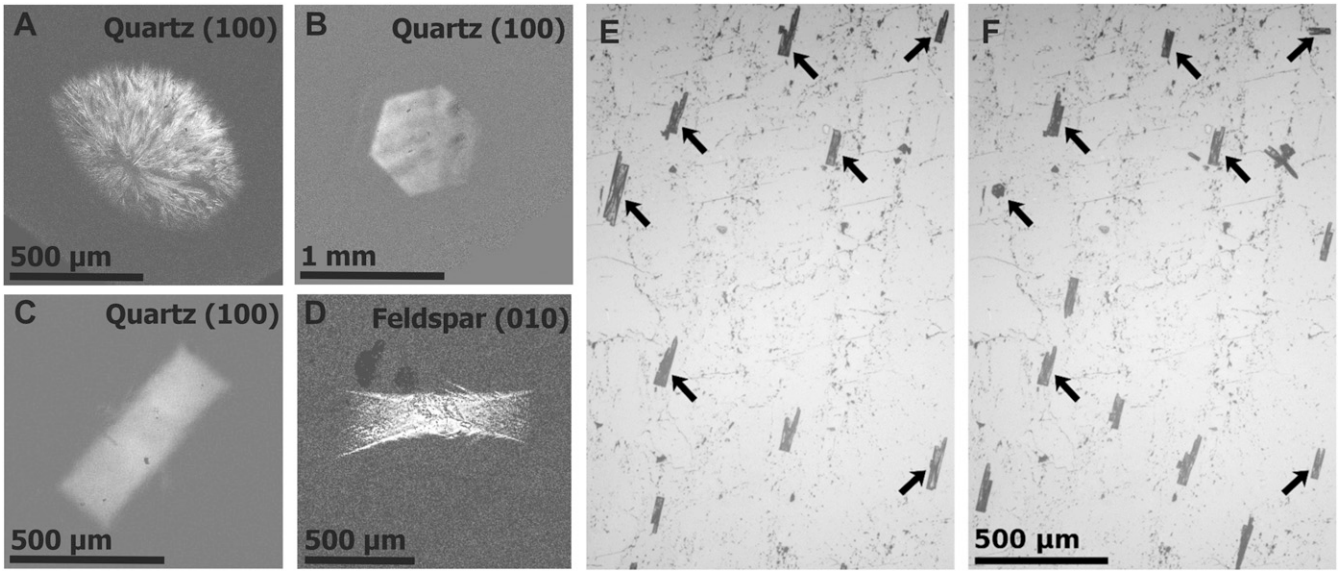

Fig. 2. Optical micrographs from immersion freezing and deposition experiments. (*A*–*D*) Immersion ice freezing showing (*A*) spherical, (*B*) hexagonal, and (*C*) rectangular morphology on the quartz (100) face and (*D*) rectangular morphology on the feldspar (010) face. Images are obtained by subtraction from an image just prior to nucleation. Note that in all cases, the growing crystal is a large number of narrow dendrites rather than a continuous solid. (*E* and *F*) Deposition ice growth on (010) feldspar on two consecutive cycles on the same region. Black arrows indicate sites that produced an ice crystal on both cycles. Note that images in both modes have been cropped and that the experimental fields of view were much larger.

A quantitative analysis of this observation is shown in Fig. 3*A*. This observation mirrors immersion freezing nucleation, where the density of active sites is known to increase as temperature decreases (23).

There was a strong epitaxial orientation of ice crystals on feldspar (Fig. 2 *E* and *F*), although not every crystal was aligned with the dominant orientation. This orientation was consistent with that previously seen by Kiselev et al. (26). It was also, significantly, in agreement with the orientation seen in the immersion freezing experiments, suggesting that similar crystallographic features of the surface promote nucleation in each mode and hinting at a common mechanism between the two modes. Individual sites often produced a crystal aligned with the dominant orientation on one cycle and unaligned the next, or vice versa; a previous study has shown that this may be the result of distinct closely spaced active sites within a single larger feature (25). Quartz in the deposition experiments did not produce a dominant alignment, again in common with immersion freezing experiments; most crystals were polycrystalline, and those which were single crystals did not display any clear common alignment.

In order to study the repeatability of the nucleation site distribution between two cycles *A* and *B*, we introduce a correlation coefficient c_{AB}, defined by the following:

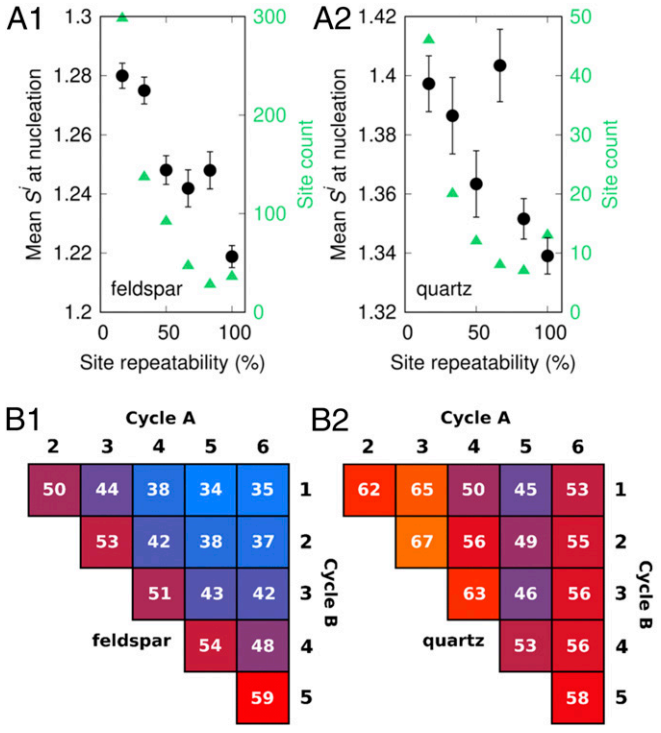

Fig. 3. (*A*) Analysis of deposition nucleation site specificity. The graphs show site statistics across all regions, binned by the site repeatability (the percentage of the six cycles on which a crystal was observed at the site). Green triangles show the number of sites within each bin. More repeatable sites were rarer but had a lower mean saturation at nucleation (black circles). Error bars represent SE on the mean. (*B*) Correlation plots demonstrating repeatability. Numbering the six experimental cycles performed on each region 1 to 6, these charts show the correlation c_{AB} between each possible combination of cycle numbers A and B calculated collectively across all regions and expressed as a percentage. On feldspar, consecutive cycles were seen to share in common a larger proportion of nucleation sites than did those separated by several intervening cycles, implying that the nucleation properties of the material changed with time. For quartz, there is no evidence of a similar trend. Statistical significance for each c_{AB} is ±3 percentage points for feldspar and ±7 points for quartz.

$$c_{AB} = \frac{N_{AB}}{\frac{1}{2}(N_A + N_B)}, \quad [1]$$

where N_A and N_B represent the total number of nucleation events on cycles *A* and *B*, respectively, and N_{AB} is the number of nucleation sites common to both cycles. Hence, c_{AB} scales from 0% (nucleation at completely different sites each cycle, that is, random distribution across the surface) to 100% (nucleation at exactly the same sites each cycle). c_{AB} was used to compare the repeatability of sites between consecutive cycles to the repeatability of sites between nonconsecutive cycles. Numbering the six experimental cycles performed on each area from one to six, we calculate c_{AB} for each combination (collectively across all substrates) as shown in Fig. 3*B*. Mean c_{AB} is 56% for quartz and 45% for feldspar. In the case of feldspar, it is clear that consecutive cycles have a stronger correlation between their sites than do cycles separated by many intervening cycles. This implies that some sites become less effective with the passage of time and/or other sites become more effective. The physical explanation for this is unclear but could relate to a weathering or aging effect caused by repeated crystallization in the same location. A susceptibility to aging has been observed in some feldspars (19). No similar trend was seen for quartz, outside statistical uncertainties. This may relate to the surface already being highly weathered due to the different preparation method, with the nucleation temperatures recorded in these experiments already reduced compared to freshly milled quartz (18, 28).

In order to test whether deposition nucleation site selection is dependent on the frost point of the vapor, additional experiments were performed on a separate feldspar substrate with 12 repeat cycles carried out at each of three different frost points (Fig. 4). Examination of c_{AB} between consecutive cycles shows that there was a relatively strong correlation of about 40% between nucleation sites at the highest frost point studied (−25 °C) but that this dropped to about 10% at the lower frost points, suggesting that the number of active sites is higher, and nucleation is less specific in colder, less humid conditions. This change in site correlation may be related to the pore condensation nucleation mechanism, which we discuss later. The lowest frost point is likely to be cold enough that homogeneous nucleation is taking place within pores; the middle frost point may also potentially feature homogeneous nucleation if negative pressure within small pores causes a significant enhancement of nucleation rate (29). We also note that when results for all three frost points are considered collectively, nucleation appears to occur almost exclusively within potassium-rich rather than sodium-rich regions of the feldspar (Fig. 4). This is in agreement with previously reported observations of immersion freezing nucleation on substrates taken from the same piece of feldspar (22).

Comparison of Immersion Freezing and Deposition. The two types of experiments produced dissimilar types of data. For immersion freezing, the growth rate of crystals was very high compared to the timescale of the experiment, such that only one nucleation site was ever observed per cycle. For deposition, the growth rate was very small compared to the experimental timescale, such that a selection of nucleation sites–some having lower onset supersaturations than others–were observed every cycle. In order to compare these two dissimilar datasets, a ranking system was used (see *Materials and Methods* section for a detailed description). Briefly, the identified nucleation sites were ordered from the most to the least active in each mode according to the frequency of occurrence of nucleation at that site and—in deposition experiments—the supersaturation at which nucleation occurred. By pinpointing the location of these sites against the distinct pattern of defects visible on the substrates, the two sets of ranked sites could be directly compared.

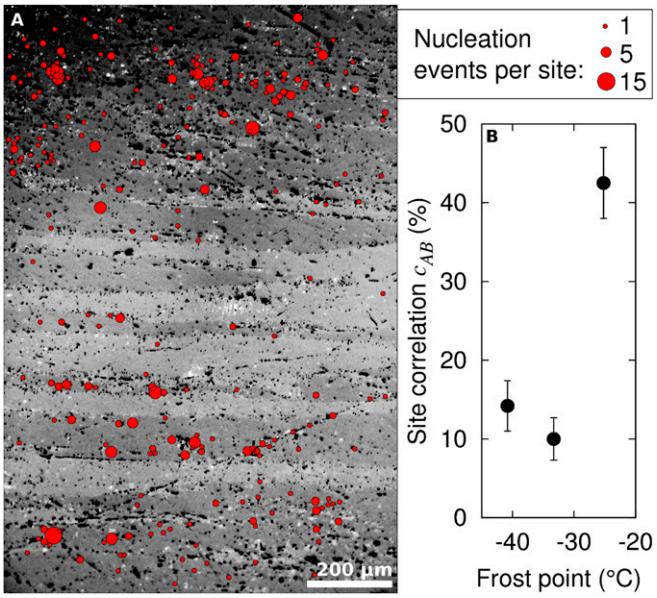

Fig. 4. (*A*) Contrast-enhanced reflected-light image of the feldspar thin section showing darker and lighter horizontal bands corresponding to potassium-rich and sodium-rich feldspar, respectively (20). Red circles show deposition nucleation sites with the area of each circle proportional to the number of cycles on which a site was active out of 36 cycles across three frost points. There is a clear preference for the potassium regions. (*B*) Mean correlation of nucleation sites between consecutive cycles as a function of the frost point. Error bars represent statistical significance.

Fig. 5 shows comparisons between the two modes for four regions; the remaining 13 areas of comparison are presented in *SI Appendix*, Figs. S2–S4. Although there were a few examples of high-ranking nucleation sites being common to both modes, such as in Fig. 5 *A* and *C*, the more typical result was for there to be little or no correlation between the two sets of sites, such as in Fig. 5 *B* and *D*.

For feldspar, 44 active immersion freezing sites were identified across all experiments, of which only three were also active deposition sites. These sites were the second ranked freezing site and the second ranked deposition site in *SI Appendix*, Fig. S2*C*, the first ranked freezing and deposition sites in Fig. 5*A*, and the second ranked freezing site and the 11th ranked deposition site in *SI Appendix*, Fig. S3*C*. Two matching sites were on the (010) face, and one was on the (001) face.

For quartz, 34 active sites were identified for immersion freezing nucleation, of which five were outside the sample area of deposition experiments. Of the remaining 29, three were also active sites for deposition nucleation. Two of these matching sites were from the same droplet, where the first ranked freezing site matched with the second ranked deposition site and vice versa in Fig. 5*C*. The third site that matched was the first ranked freezing site and the seventh ranked deposition site in *SI Appendix*, Fig. S4*C*.

Across all substrates, this gives a total of six out of 73 active sites for immersion freezing that were also among the 337 ranked active sites for deposition. This is a coincidence rate of just 8%, which is extremely low compared to the values between 66% and 84% recorded for the coincidence between cycles of immersion freezing and deposition individually. This clearly demonstrates that nucleation principally occurs in different sites in immersion freezing and deposition modes. However, it also shows that there can be some correlation in nucleation sites between the two modes. It might be expected that a few false-positive matches between sites could occur if they are too closely spaced to be distinguished within our experimental resolution. However, we would not expect this to be as much as 8% if the two modes were entirely uncorrelated, as significantly less than 8% of the surface area is within experimental uncertainty of a ranked deposition nucleation site (Fig. 5). The 8% coincidence becomes more significant if we notice that the few sites in which there was agreement between the two modes of nucleation were almost exclusively highly ranked sites for each mode. The mean rank of matching sites (across both feldspar and quartz) was 1.5 for immersion freezing and 4 for deposition compared to the mean rank for all comparable sites of 2.9 for immersion freezing and 20.6 for deposition. Although we cannot draw firm conclusions from as few data as six matching sites, the suggestion is that the most active sites in each mode are the most likely to also be active in the other and that as we sample higher densities of decreasingly active sites, the correlation between the two modes also decreases. The much firmer conclusion from our data, however, is simply that certain sites can be active in both immersion freezing and deposition nucleation but that it is much more common that they are not.

Discussion

To be sure that the observed preference for certain nucleation sites is significant, we must satisfy ourselves that it is the result of a true preference for nucleation rather than the result of ice embryos being retained within confined geometries between cycles, acting as a seed on subsequent cycles. To prevent this, all substrates in both modes were warmed to +5 °C between each cycle, and the success of this may be judged from the data: if ice embryos retained after the first cycle were acting as seeds for subsequent cycles, we would expect those subsequent cycles to need a lower supercooling/supersaturation for crystal growth. This is not seen. For immersion freezing experiments, the nucleation temperature on the first cycle of each droplet was (mean ± SD) −13.7 ± 1.4 °C on feldspar and −19.0 ± 3.3 °C on quartz compared to −13.6 ± 1.2 °C and −20.3 ± 2.1 °C, respectively, across all cycles. For deposition, the saturation with respect to ice at the first observed crystal growth on the first cycle of each region was (mean ± SD) 1.14 ± 0.08 on feldspar and 1.29 ± 0.05 on quartz compared to 1.15 ± 0.07 and 1.30 ± 0.03, respectively, across all cycles. Site selection on the first cycle was also similar to that of other cycles. Fig. 3*B* show that the site correlation c_{AB} between the first and subsequent cycles was similar to that between other cycles on both materials, and *SI Appendix*, Figs. S7–S9 do not suggest that first-cycle site selection is atypical for immersion freezing.

Before we can meaningfully interpret the differences between deposition and immersion freezing nucleation sites, we must answer the following question: are our deposition experiments suggestive of a pore condensation and freezing nucleation mechanism? Deposition ice nucleation was seen to occur below water saturation on feldspar, in common with previous experiments (25, 30). The average water saturation of 0.93 at first nucleation is sufficient to fill pores of up to 34 nm diameter (from the Kelvin equation assuming hydrophilic cylindrical pores). Scanning electron and atomic force microscopy studies of feldspar surfaces have shown that there are many submicron pores and cracks (22, 25), and although the resolution in these studies was not quite sufficient to resolve features of 34 nm diameter or below, their presence seems highly likely. A previous study also showed that deposition nucleation sites of ice on feldspar are strongly correlated with surface sites where sub-100 nm pores are present (25). Scanning electron microscopy of polished quartz has also identified submicron surface geometries (22), although at a lower concentration than on feldspar surfaces, and it is uncertain whether our unpolished facets would display similar features. Our average water saturation at first nucleation on quartz, 0.98, equates to pores of 125 nm diameter, so much wider pores could have been filled than on feldspar. Altogether, deposition nucleation on feldspar and quartz is strongly suggestive of pore condensation and freezing.

We might therefore expect that there should be some degree of correlation between sites in the two modes. At temperatures

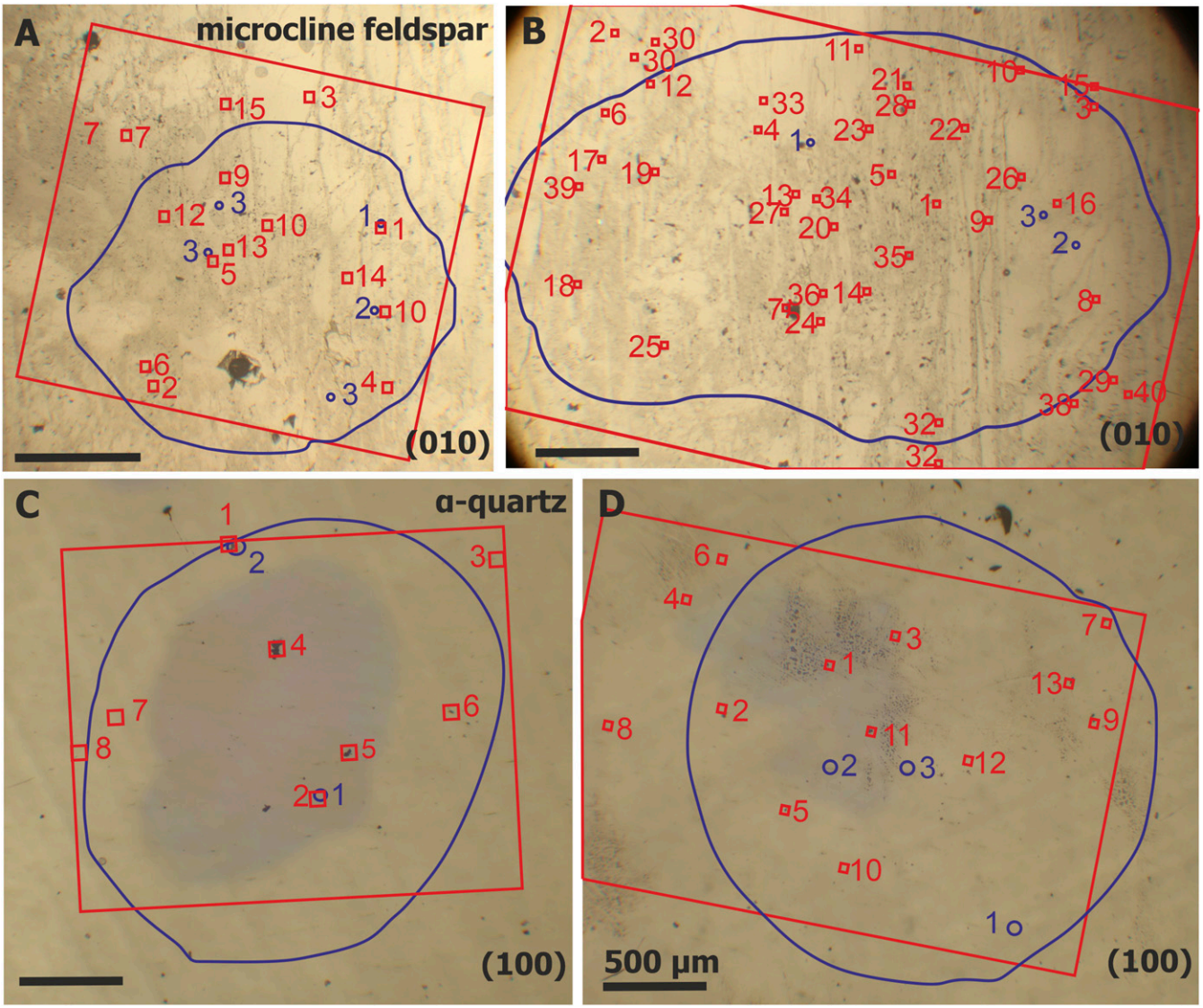

Fig. 5. Example comparisons of ranked nucleation sites on (*A* and *B*) (010) feldspar and (*C* and *D*) (100) quartz. The red squares mark the deposition sites, and the blue circles mark the immersion freezing sites, superimposed on optical micrographs of the substrates. The size of each symbol represents the uncertainty in site position. In each case, site number one is the most effective and so on. The red rectangle marks the analyzed region in deposition experiments, and the blue line marks the initial wetted area of the droplet in immersion freezing experiments. The black lines are 500 μm scale bars. *A* and *C* show atypical results, where there is good agreement between the most effective sites in the two modes; *B* and *D* show more typical results with no correlation between the two sets of sites.

above those relevant for homogeneous freezing, an effective pore for condensation and freezing must contain a good nucleation site for the freezing of water, and therefore it should also be an effective site for immersion freezing. We observe several things that support the hypothesis that immersion freezing and deposition nucleation operate by a common mechanism. Both modes produce crystals with a common epitaxial alignment on feldspar, implying a similar strong influence of one or more specific crystal planes present at active sites; neither mode appears to involve epitaxy on quartz. Deposition nucleation occurs preferentially in potassium-rich areas of feldspar, just as has been observed with immersion freezing previously. And the increasing number of deposition active sites with decreasing frost points is to be expected if pores are filling with water and then freezing; whereas at higher temperatures, only a few pores will contain a nucleation site, allowing the water to freeze, at lower temperatures, a wider range of nucleation sites will become available (until below the homogeneous nucleation temperature, when all pores which can condense water can produce ice crystals).

Why then, at temperatures too high for homogeneous nucleation of ice, is there a poor correlation between the active sites for deposition and immersion freezing? We cannot definitively answer this question, but we present five possible explanations with a discussion of each.

The first possibility is that the best immersion freezing sites are not necessarily within pores where capillary condensation can take place and therefore are not effective for pore condensation and freezing. It has been shown that immersion freezing active sites on feldspar are correlated with submicron surface features (22), but whether or not they are generally within sufficiently narrow features to allow capillary condensation within our experimental conditions is unknown.

We must also consider a second possibility that water in the immersion freezing experiments does not always penetrate down to the very bottoms of the pores due to trapped air pockets, following the Cassie–Baxter model (31). This would mean that some nucleation sites which are active for deposition nucleation are not available for immersion freezing nucleation. Recent

studies comparing different ice nucleation measurement techniques have suggested that the method by which a droplet is formed in an immersion freezing experiment can influence the freezing temperature measured (32, 33). Bringing liquid water into contact with a dry surface may trap air pockets, limiting access to nucleation sites. In our freezing experiments, we attempted to mitigate against air pocket formation by lowering the surface temperature to 4 °C such that water condensed on the surface before the droplets were pipetted on, presumably filling up any small cavities. The condensed water on the surface around the droplet was then evaporated off by applying a nitrogen atmosphere. However, we cannot completely rule out the formation of small air pockets.

A third possibility is solute effects. In heterogeneous systems such as minerals, trace concentrations of many elements are present. The influence of even low concentrations of solutes on ice nucleation temperature can be large, with ammonium known to enhance ice nucleation, while other salts can suppress freezing (34–36). Very high concentrations could quickly accumulate in capillary condensates within pores because of their large surface to volume ratios. Different pores would accumulate different concentrations of different solutes, depending on their chemistry and geometry. The same effect would be insignificant within the bulk droplet used in immersion freezing experiments, leading to a variation between the two modes.

A fourth explanation for the low correlation between sites could lie in the lower temperatures in deposition experiments compared to immersion freezing experiments. This could have led to a wider range of freezing sites being active in deposition experiments than in immersion freezing experiments, although it seems reasonable to assume that the active sites identified in immersion freezing experiments should remain extremely active at the lower temperatures used in deposition experiments.

Finally, it is possible that some nucleation sites that are effective for immersion freezing would be ineffective for deposition because they are in excessively narrow pores. There is an energy barrier associated with the growth of confined ice into a bulk crystal through a very narrow pore mouth (12, 14, 37), and this barrier would be much higher in air than in water due to the higher ice-vapor than ice-water surface energy. Thus, a capillary condensate might freeze within a pore which is highly active but be unable to grow out until a high supersaturation is reached.

It is significant, however, that despite all these reasons to expect differences between the two modes, a few regions exhibited nucleation sites which were active for both immersion freezing and deposition. Therefore, although an effective nucleation site in one mode is unlikely to be an effective nucleation site in the other for the reasons suggested above, it is nevertheless possible for a single nucleation site to be highly effective in both modes. In these cases, it is likely that an active site available for freezing is present within a pore suitable for the two-step pore condensation mechanism.

Our findings should be directly applicable to clouds containing feldspar and quartz aerosol particles under conditions where the ice nucleation site densities are around 1 per square millimeter. Further work would be needed to explore much larger and smaller active-site densities. However, the general finding of this work should be much more broadly applicable: that the nucleating ability of aerosols for immersion freezing and for deposition—although not uncorrelated—must be considered separately.

Conclusion

In the search for greater understanding of ice nucleation processes, we are faced with an unassailable challenge: that the surface sites within which nucleation occurs are only a few nanometers in size. This is much too small to observe the process directly with any presently known experimental techniques, although microscopists continue to make strides in the molecular imaging of ice and of transient phenomena, which may one day lead us to that goal (38, 39). However, for now, we are forced to glean knowledge of the mechanism of nucleation indirectly, through the study of the crystals which result from it. We have made careful study of the locations of crystals grown on thin sections of two important atmospheric nucleants—feldspar and quartz—and confirmed the finding of earlier studies that nucleation is far from random but instead is dominated by a small number of active sites on the surface. This finding holds for both of the atmospherically relevant modes of ice nucleation: immersion freezing and deposition. The key uncertainty we wished to address was the relationship between the two modes, that is., whether or not a nucleant being effective in one mode would imply it also being effective in the other or whether it is possible for a surface to be an effective nucleant in one mode yet ineffective in the other. This was addressed primarily through comparing the locations of active sites between each mode. Across 17 areas studied in both freezing and deposition experiments, only four areas exhibited any correlation at all between any of their active sites.

This low correlation provides strong evidence that the fundamental requirements for an effective nucleation site differ between the two modes. This is an interesting finding in light of theories of deposition nucleation being explained by condensation and freezing within narrow pores, since this implies that an effective nucleation site for deposition should also be effective for immersion freezing. We propose, however, that the converse is not true, since an effective site for pore condensation and freezing has additional requirements beyond just being an effective site for freezing nucleation: the freezing site must be inside a pore narrow enough for water to condense but not too narrow to prevent growth into a bulk crystal, and the chemistry and geometry of the pore must not lead to high concentrations of nucleation-inhibiting solute within the condensate. This demonstration of the role of the geometry of the surface, rather than just surface chemistry, is consistent with a growing body of evidence that highlights the importance of surface topography in controlling nucleation (12, 14, 20, 22, 25, 40). Greater understanding of the role of both chemistry and topography in nucleation will not only help us to understand and model atmospheric processes but may also inform new strategies for designing surfaces to control nucleation, such as anti-icing surfaces, which need to be manufactured to prevent ice formation both from liquid droplets and from water vapor (41–43).

Materials and Methods

Two samples of alkali feldspar (potassium-rich microcline containing veins of sodium-rich albite) were used, which we refer to as LD6 and LD7. Petrographic thin sections were prepared on glass slides and sequentially polished to 30 μm thickness along the (010) and (001) faces, one for each face for each sample. Polarized light micrographs from each crystal face are shown in *SI Appendix*, Fig. S5, characterizing the samples as microcline and demonstrating the sodium-rich and potassium-rich regions. Two or three regions were studied on each thin section, giving 11 regions in total. Deposition experiments on the frost-point dependence of active sites were performed on one (001) thin section of feldspar LD3, which has been previously studied in immersion freezing experiments (19, 20, 22). Feldspar was obtained from the University of Leeds mineral collection and verified using powder X-ray diffraction (XRD) and cross-polarized light microscopy (*SI Appendix*, Figs. S5 and S6).

Quartz substrates were prepared in a different way, using a natural facet surface from a euhedral single crystal rather than a polished anhedral surface, such as the rose quartz used by Holden et al. (22). Therefore, the surface was free from polishing lines, which could have otherwise assisted condensation of water in deposition experiments. Three single crystals of quartz were embedded with a (100) face set in wax and then sawn and polished down to a 1 mm thick substrate. The wax was then removed from the facet surface, soaking twice overnight in toluene and rinsing in ethanol to remove traces of wax. Two regions were studied on each substrate, giving six regions in total. Quartz crystals were obtained from a private seller and verified using Raman spectroscopy and powder XRD (*SI Appendix*, Fig. S6).

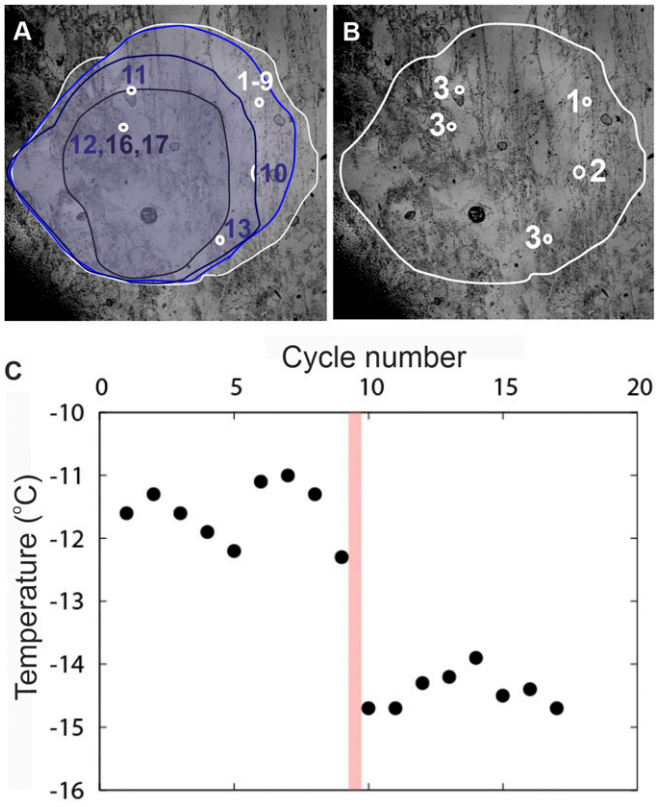

Fig. 6. A demonstration of the site ranking system for immersion freezing experiments. The optical micrograph in *A* indicates the location of all nucleation events labeled by cycle number. Note that cycles 14 and 15 are omitted since the nucleation site could not be identified with sufficient resolution. The lines show the moving position of the droplet perimeter because of evaporation: from white to dark blue, these correspond to cycles 0, 5, 10, and 15. (*B*) The final ranking given to the active sites. (*C*) The nucleation temperatures recorded over the experiment. The pink line indicates the point at which the most effective site (ranked 1) is removed from the droplet due to evaporation.

Both feldspar and quartz substrates were rinsed in isopropanol and water prior to each set of experiments for both immersion freezing and deposition. Freezing experiments were performed before deposition experiments.

Immersion Freezing Experiments. Immersion freezing experiments were performed using a high-speed video microscopy setup previously described by Holden et al. (22). A 1 μl droplet of water was pipetted onto the surface, and the temperature decreased at 10 °C/min until freezing was observed. At this point, the high-speed camera was triggered, capturing the preceding 1 s of video and allowing the identification of the region in which nucleation occurred. The nucleation temperature was also recorded. In one experiment (*SI Appendix*, Fig. S7*A*), the temperature was decreased at 1 °C/min rather than 10 °C/min in cycles 1 to 17 and 19 to 24. The temperatures recorded in these cycles were not included in the average freezing temperature calculations because the cooling rate will affect the freezing temperature. Once the video was recorded, the stage was heated to +5 °C to thaw the droplet before restarting another cycle. In total, 11 to 37 cycles were performed per region. The high ramp rate of 10 °C/min was selected in order to increase the chances of observing nucleation at a higher number of active sites over the course of the experiment. A zero-grade nitrogen flow was used to prevent condensation around the droplet. The flow rate was varied between 100 and 500 sccm (standard cubic centimeters per minute).

Complementary freezing experiments were performed using arrays of 1 μL droplets on the feldspar and quartz surfaces. At least two separately prepared surfaces were used for each crystal face investigated. A minimum of 49 total droplets were frozen on each crystal face. The droplet arrays were cooled using the microliter Nucleation by Immersed Particles Instrument (44). The surfaces were placed on a cryocooler and cooled from +15 to −40 °C at 1 °C/min. A Perspex cell was placed around the array and zero-grade nitrogen was flowed at 300 sccm to prevent condensation. Freezing events were identified optically using a webcam, and corresponding temperatures were recorded.

The active-site density, $n_s(T)$, was used to compare the ice nucleation effectiveness of the monolithic substrates to typical ground feldspar and quartz samples. This is an approximation that assumes that nucleation is singular, meaning that ice nucleation sites become active at a specific temperature, and is calculated as

$$\frac{n(T)}{N} = 1 - \exp(-n_s(T)A), \quad [2]$$

where n(T) is the number of droplets frozen at temperature T, N is the total number of droplets in the experiment, and A is the surface area per droplet. The average surface area covered by a 1 μL water drop on a surface is 0.045 ± 0.009 cm^2 for feldspar and 0.041 ± 0.006 cm^2 for quartz. The uncertainties in $n_s(T)$ were calculated by propagating the surface area measurement uncertainties with the Poisson uncertainties as described in Harrison et al. (19).

Deposition Experiments. Deposition experiments were performed in a humidity-controlled microscopical cooling stage. The area of observation could be aligned with that of the immersion freezing experiments by reference to the pattern of defects visible within the mineral. Gas flow through the chamber was maintained at a constant water vapor content while the substrate temperature was decreased at 1 °C/min until crystals were seen growing. The experiment was continued for 1.5 °C after observation of the first crystal seen within the area of interest; all crystals nucleating after this arbitrary cutoff are excluded from all statistics. Six repeat cycles were performed for each region, with the temperature taken up above +5 °C between cycles to remove the possibility of retained ice embryos influencing results. For the experiment with varying frost points, a slightly different protocol was used, with the first 12 nucleation sites on each cycle being used as the basis for statistics and 12 cycles being performed for each frost point.

The frost point of the vapor (the temperature at which it would be in equilibrium with ice) was measured typically after the third cycle by heating the substrate at 0.1 °C/min to find the temperature at which the crystals were neither growing nor shrinking. For feldspar, measured frost points were between −20.2 and −21.5 °C. In the case of quartz, these conditions were not sufficient to trigger ice nucleation prior to reaching water saturation, leading to bulk condensation across the surface followed by freezing. Therefore, drier conditions were used, with measured frost points between −25.4 and −26.3 °C.

All stated temperatures carry an absolute error of ±0.3 °C for deposition experiments and ±0.4 °C for immersion freezing experiments, and all saturations have an absolute error of ±0.02.

Ranking of Nucleation Sites. In immersion freezing experiments, ice nucleation was immediately followed by rapid crystal growth so that only one site was observed per freeze–thaw cycle. The number of nucleation events observed at each site over the course of a multicycle experiment was used to rank the effectiveness of a site. As the droplet gradually evaporated over the course of the experiment, the contact line would sometimes recede beyond an active site, leaving it outside the droplet on subsequent cycles. In order to counteract sampling bias as much as possible, when this occurred, the ranking of site effectiveness was restarted, with sites already identified being assigned a rank and excluded from further testing.

An illustrative example is shown in Fig. 6 with all analysis shown in *SI Appendix*, Figs. S7–S9. In Fig. 6, the most active site is where ice nucleated in the first nine cycles. At the start of the 10th cycle, the first site had been removed from the droplet. This was given rank 1. No other sites had yet to be identified, and the experiment was continued. In cycle 10, a second site was identified. However, this was outside the droplet by cycle 11, and so it was given rank 2, and the ranking process was restarted. Between cycles 11 and 13, three sites were identified, each of which nucleated ice once. Nucleation was observed at the contact line in cycles 14 and 15, where the nucleation site could not be identified with sufficient resolution; these were therefore excluded from processing. After cycle 14, the nucleation site in cycle 13 was no longer in the droplet. Therefore, the three sites observed were each given the same rank—3—and excluded from further testing. The final two cycles, 16 and 17, had nucleation at the site identified in cycle 12. However, this did not affect ranking as this site had already been ranked and excluded.

In deposition experiments, a large number of crystals were seen on each cycle. Two criteria were therefore considered for ranking nucleation sites: the number of cycles on which a crystal nucleated at a site and the saturation at which those crystals nucleated. These criteria are not entirely independent, as sites that nucleated crystals more often also tended to nucleate crystals at

lower supersaturations (Fig. 3). In order to account for both statistics in our ranking, each site was awarded a score for each cycle on which a crystal appeared, equal to:

$$10^{T_n - T_0}, \quad [3]$$

where T_n is the temperature (in °C) at which the crystal appeared, and T_0 is the temperature at which the first crystal appeared within the region of interest. Thus, the first site to host a crystal on any cycle receives a score of 1, while a site without a crystal until 1 °C after the first crystal receives a score of 0.1, etc. To reduce the large number of sites in consideration, only sites which nucleated crystals on two or more cycles out of six—or hosted the first nucleation event of a cycle—are included in the rankings.

Data Availability. Comma-separated value files containing all data used to construct the plots have been deposited in the Research Data Leeds Repository (https://doi.org/10.5518/926).

ACKNOWLEDGMENTS. We thank J. Harri Wyn Williams for preparing petrographic thin section samples, Lesley Neve for assistance with XRD measurements, and Grace Porter for assistance with uncertainty analysis. This project was supported by the Engineering and Physical Sciences Research Council (EPSRC) Grants EP/M003027/1 (H.K.C., F.C.M., B.J.M., and M.A.H.) and EP/N002423/1 (F.C.M., H.K.C., and M.A.H.), an EPSRC Programme grant which funds the Crystallisation in the Real World consortium EP/R018820/1 (F.C.M.), the Leverhulme Trust RPG-2014-306 (H.K.C. and J.M.C.), and the European Research Council 648661 Marinelce (B.J.M.).

1. I. Tan, T. Storelvmo, M. D. Zelinka, Observational constraints on mixed-phase clouds imply higher climate sensitivity. *Science* **352**, 224–227 (2016).
2. J. Vergara-Temprado *et al*., Strong control of Southern Ocean cloud reflectivity by ice-nucleating particles. *Proc. Natl. Acad. Sci. U.S.A.* **115**, 2687–2692 (2018).
3. A. V. Matus, T. S. L'Ecuyer, The role of cloud phase in Earth's radiation budget. *J. Geophys. Res. Atmos.* **122**, 2559–2578 (2017).
4. A. J. Heymsfield *et al*., Cirrus clouds. *Meteor. Mon.* **58**, 2.1–2.26 (2017).
5. B. J. Murray, K. S. Carslaw, P. R. Field, Opinion: Cloud-phase climate feedback and the importance of ice-nucleating particles. *Atmos. Chem. Phys.* **21**, 665–679 (2021).
6. B. J. Murray, D. O'Sullivan, J. D. Atkinson, M. E. Webb, Ice nucleation by particles immersed in supercooled cloud droplets. *Chem. Soc. Rev.* **41**, 6519–6554 (2012).
7. Z. A. Kanji *et al*., Overview of ice nucleating particles. *Meteor. Mon.* **58**, 1.1–1.33 (2017).
8. N. Fukuta, Activation of atmospheric particles as ice nuclei in cold and dry air. *J. Atmos. Sci.* **23**, 741–750 (1966).
9. C. Marcolli, Deposition nucleation viewed as homogeneous or immersion freezing in pores and cavities. *Atmos. Chem. Phys.* **14**, 2071–2104 (2014).
10. R. O. David *et al*., Pore condensation and freezing is responsible for ice formation below water saturation for porous particles. *Proc. Natl. Acad. Sci. U.S.A.* **116**, 8184–8189 (2019).
11. H. K. Christenson, Two-step crystal nucleation via capillary condensation. *CrystEngComm* **15**, 2030–2039 (2013).
12. J. M. Campbell, F. C. Meldrum, H. K. Christenson, Observing the formation of ice and organic crystals in active sites. *Proc. Natl. Acad. Sci. U.S.A.* **114**, 810–815 (2017).
13. H. R. Pruppacher, J. D. Klett, *Microphysics of Clouds and Precipitation* (Springer Netherlands, Dordrecht, 2010), pp. 287–360.
14. J. M. Campbell, H. K. Christenson, Nucleation- and emergence-limited growth of ice from pores. *Phys. Rev. Lett.* **120**, 165701 (2018).
15. J. D. Atkinson *et al*., The importance of feldspar for ice nucleation by mineral dust in mixed-phase clouds. *Nature* **498**, 355–358 (2013).
16. J. D. Yakobi-Hancock, L. A. Ladino, J. P. D. Abbatt, Feldspar minerals as efficient deposition ice nuclei. *Atmos. Chem. Phys.* **13**, 11175–11185 (2013).
17. D. J. Cziczo *et al*., Clarifying the dominant sources and mechanisms of cirrus cloud formation. *Science* **340**, 1320–1324 (2013).
18. A. D. Harrison *et al*., The ice-nucleating ability of quartz immersed in water and its atmospheric importance compared to K-feldspar. *Atmos. Chem. Phys.* **19**, 11343–11361 (2019).
19. A. D. Harrison *et al*., Not all feldspars are equal: A survey of ice nucleating properties across the feldspar group of minerals. *Atmos. Chem. Phys.* **16**, 10927–10940 (2016).
20. T. F. Whale *et al*., The role of phase separation and related topography in the exceptional ice-nucleating ability of alkali feldspars. *Phys. Chem. Chem. Phys.* **19**, 31186–31193 (2017).
21. T. Zolles *et al*., Identification of ice nucleation active sites on feldspar dust particles. *J. Phys. Chem. A* **119**, 2692–2700 (2015).
22. M. A. Holden *et al*., High-speed imaging of ice nucleation in water proves the existence of active sites. *Sci. Adv.* **5**, eaav4316 (2019).
23. G. Vali, Interpretation of freezing nucleation experiments: Singular and stochastic; sites and surfaces. *Atmos. Chem. Phys.* **14**, 5271–5294 (2014).
24. M. J. Wheeler *et al*., Immersion freezing of supermicron mineral dust particles: Freezing results, testing different schemes for describing ice nucleation, and ice nucleation active site densities. *J. Phys. Chem. A* **119**, 4358–4372 (2015).
25. E. Pach, A. Verdaguer, Pores dominate ice nucleation on feldspars. *J. Phys. Chem. C* **123**, 20998–21004 (2019).
26. A. Kiselev *et al*., Active sites in heterogeneous ice nucleation-the example of K-rich feldspars. *Science* **355**, 367–371 (2017).
27. C. L. Ryder *et al*., Coarse-mode mineral dust size distributions, composition and optical properties from AER-D aircraft measurements over the tropical eastern Atlantic. *Atmos. Chem. Phys.* **18**, 17225–17257 (2018).
28. A. Kumar, C. Marcolli, T. Peter, Ice nucleation activity of silicates and aluminosilicates in pure water and aqueous solutions–Part 2: Quartz and amorphous silica. *Atmos. Chem. Phys.* **19**, 6035–6058 (2019).
29. C. Marcolli, Ice nucleation triggered by negative pressure. *Sci. Rep.* **7**, 16634 (2017).
30. F. Zimmermann *et al*., Ice nucleation properties of the most abundant mineral dust phases. *J. Geophys. Res. Atmos.* **113** (2008).
31. A. B. D. Cassie, S. Baxter, Wettability of porous surfaces. *Trans. Faraday Soc.* **40**, 546–551 (1944).
32. N. Hiranuma *et al*., A comprehensive laboratory study on the immersion freezing behavior of illite NX particles: A comparison of 17 ice nucleation measurement techniques. *Atmos. Chem. Phys.* **15**, 2489–2518 (2015).
33. N. Hiranuma *et al*., A comprehensive characterization of ice nucleation by three different types of cellulose particles immersed in water. *Atmos. Chem. Phys.* **19**, 4823–4849 (2019).
34. A. Kumar, C. Marcolli, B. Luo, T. Peter, Ice nucleation activity of silicates and aluminosilicates in pure water and aqueous solutions–Part 1: The K-feldspar microcline. *Atmos. Chem. Phys.* **18**, 7057–7079 (2018).
35. T. F. Whale, M. A. Holden, T. W. Wilson, D. O'Sullivan, B. J. Murray, The enhancement and suppression of immersion mode heterogeneous ice-nucleation by solutes. *Chem. Sci. (Camb.)* **9**, 4142–4151 (2018).
36. M. T. Reischel, G. Vali, Freezing nucleation in aqueous electrolytes. *Tellus* **27**, 414–427 (1975).
37. A. J. Page, R. P. Sear, Heterogeneous nucleation in and out of pores. *Phys. Rev. Lett.* **97**, 065701 (2006).
38. M. Mehlhorn, S. Schnur, A. Groß, K. Morgenstern, Molecular-scale imaging of water near charged surfaces. *ChemElectroChem* **1**, 431–435 (2014).
39. G. Bakradze, K. Morgenstern, Temperature-dependent shape changes of ice nanoclusters on Ag (100). *ChemPhysChem* **19**, 2858–2862 (2018).
40. Y. Bi, B. Cao, T. Li, Enhanced heterogeneous ice nucleation by special surface geometry. *Nat. Commun.* **8**, 15372 (2017).
41. S. Nath, S. F. Ahmadi, J. B. Boreyko, A review of condensation frosting. *Nanosc. Microsc. Therm. Eng.* **21**, 81–101 (2017).
42. O. Parent, A. Ilinca, Anti-icing and de-icing techniques for wind turbines: Critical review. *Cold Reg. Sci. Technol.* **65**, 88–96 (2011).
43. M. J. Kreder, J. Alvarenga, P. Kim, J. Aizenberg, Design of anti-icing surfaces: Smooth, textured or slippery? *Nat. Rev. Mater.* **1**, 15003 (2016).
44. T. F. Whale *et al*., A technique for quantifying heterogeneous ice nucleation in microlitre supercooled water droplets. *Atmos. Meas. Tech.* **8**, 2437–2447 (2015).